JOURNAL OF MATERIALS SCIENCE 18 (1983) 753–758

The effect of aluminium on mechanical properties and thermal stability of (Fe, Ni)–Al–P ternary amorphous alloys

A. INOUE, A. KITAMURA*, T. MASUMOTO
The Research Institute for Iron, Steel and Other Metals, Tohoku University, Sendai 980, Japan

Amorphous phase formation with good ductility has been found in Fe–Al–P and Ni–Al–P ternary systems by using a melt-spinning technique. The aluminium content of these amorphous alloys is in the range 0 to 18 at % for the Fe–Al–P system and 0 to 6 at % for the Ni–Al–P system. Crystallization temperature and Vickers hardness increase with increasing aluminium and phosphorus content and maximum values are attained at 721 K and 640 diamond pyramid number (DPN). Their fracture strengths are about 2000 MPa. The effectiveness of aluminium on the increase in crystallization temperature is very great, being almost the same as that of silicon and the refractory metals such as vanadium, niobium, molybdenum and tungsten, but its effectiveness on the increase in hardness is not so great. From the previous data on the effect of aluminium on the activity coefficient of phosphorus in molten iron, it is inferred that the effectiveness of aluminium is due to the attractive interaction between aluminum and iron or nickel which is greater than that between aluminium and phosphorus.

1. Introduction

Aluminium–containing alloys possess high engineering potential because of their low cost as well as the ease with which their alloys may be melted and ejected. Therefore, it is very important from scientific and technological points of view to clarify the effect of aluminium on amorphous phase-forming ability, thermal stability, mechanical strength and chemical and physical properties. Recently, we have found [1] that an amorphous single phase is formed in a wide range of composition for X–Al–B (X = Fe, Co or Ni) systems and the effectiveness of aluminium on the increase in crystallization temperature and hardness is greater than that of other metal elements such as chromium, manganese, iron, cobalt and nickel. Further, it has been inferred [1] that the reason for this great effectiveness of aluminium is due to a rather strong metalloid-like character of the aluminium atom. In the subsequent investigation, we have tried to form an amorphous phase in X–Al–P (X = Fe or Ni) systems. Phosphorus as well as boron has known to be an essential metalloid element in forming an amorphous phase exhibiting useful engineering properties such as the Invar effect [2], corrosion resistance [3] and catalysis [4]. The purpose of this paper is to present the formation range, crystallization temperature, the activation energy for crystallization, hardness and tensile fracture strength of amorphous alloys in Fe–Al–P and Ni–Al–P systems and to clarify the effect of aluminium on their properties.

2. Experimental procedure

The specimens used in the present work were $Fe_{100-x-y}Al_xP_y$ and $Ni_{100-x-y}Al_xP_y$ ternary alloys. These subscripts are weighed values and represent atomic percentage. The alloy ingots were prepared from electrolytic pure metal (iron or nickel), aluminium (99.99 wt %) and Fe–26.8 wt % P or Ni–14.9 wt % P alloy in an argon induction furnace. Small pieces of the ingots were melted by using a conventional melt-spinning apparatus and

*Present address: The Patent Bureau, Tokyo 100, Japan.

0022–2461/83/030753–06$03.22/0

rapidly solidified to form a continuous ribbon which was about 0.5 to 1 mm in width and about 10 to 15 μm in thickness. The roller material used in the apparatus was steel for the iron-based alloys and copper for the nickel-based alloys. X-ray diffraction, transmission electron microscopy, differential scanning calorimetry (DSC) and differential thermal analysis (DTA) were carried out on both as-quenched and heat-treated samples, as described previously [1]. Hardness and tensile fracture strength were measured with a Vickers microhardness tester using a 100 g load and an Instron-type tensile testing machine at a strain rate of 1.67×10^{-4} sec^{-1}.

3. Results and discussion

3.1. Formation ranges of the amorphous phase

Formation of a completely amorphous phase was achieved for a wide range of compositions in the Fe–Al–P and Ni–Al–P ternary systems as shown in Figs. 1a and b. These amorphous alloys are so ductile that no crack is observed even after closely contacted bending test. The values in the figures are the crystallization temperatures determined as the starting point of the first exothermic peak on the DTA curves measured at a heating rate of 5 K min^{-1}. An amorphous phase was obtained in a range of compositions, e.g. 0 to 18 at% Al and 13 to 21 at% P for Fe–Al–P alloys and 0 to 6 at% Al and 15 to 23 at% for Ni–Al–P alloys. Amorphous phase formation in the Fe–P and Ni–P binary systems is relatively easy, whereas no amorphous phase is formed in Fe–Al and Ni–Al binary alloys. Further, one can see that the addition of aluminium results in a slight extension in phosphorus content from 15 to 13 at% for Fe–Al–P amorphous alloys, in contrast to the result that the composition range of phosphorus in Ni–Al–P amorphous alloys becomes narrow by the addition of aluminium. Thus, the formation range of an amorphous phase is much wider for the Fe–Al–P system than for the Ni–Al–P system despite the facts that the extent of the formation range of binary Fe–P and Ni–P amorphous alloys is almost the same and the melting point (T_m) is much lower for Ni–Al–P alloys than that for Fe–Al–P alloys. Although the reason for such a significant difference in their amorphous phase-forming ranges is not clear at present, it may be due to the following facts: the solubility limit

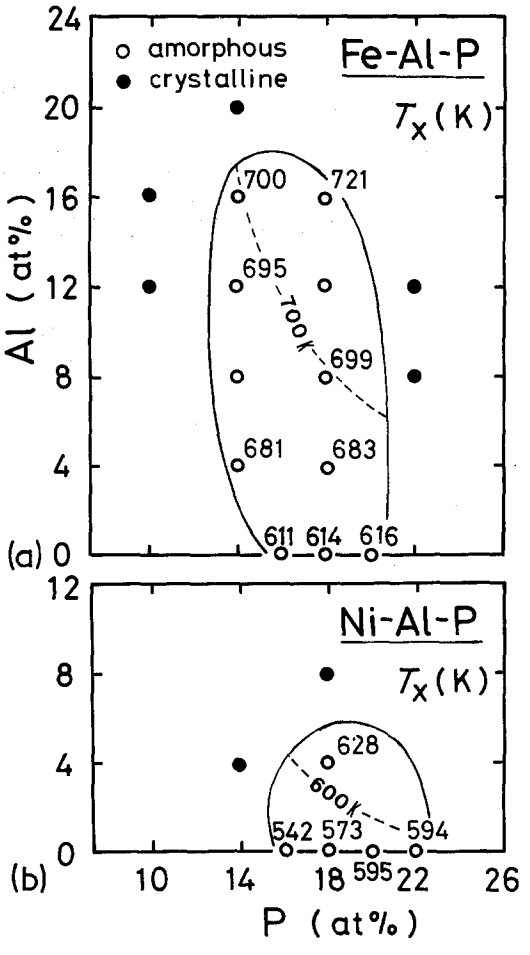

Figure 1 Composition range for the formation of amorphous phase and the change of crystallization temperature (T_x). (a) Fe–Al–P system, (b) Ni–Al–P system.

of aluminium in the Ni–P alloys is much smaller than in the Fe–P alloys because of the larger difference in atomic size between nickel and aluminium than that between iron and aluminium, resulting in an ease of the precipitation of the crystalline phase. That is, aluminium atoms are able to replace iron atoms up to about 18 at% Al in the Fe–P amorphous structure, but in the Ni–P amorphous structure the aluminium content is limted to less than about 6 at%. This assumption is also supported by the fact that the binary phase diagram is a typical eutectic type for Ni–Al alloys and a miscibility type for Fe–Al alloys. Additionally, the crystallization temperature of the Fe–Al–P alloys is higher by about 20 to 70 K than that of the Ni–Al–P alloys containing the same amounts of aluminium and phosphorus as shown in Figs. 1a and b, suggesting that glass transition temperature is

considerably higher for the former alloys than for the latter alloys. This may be another reason why the Fe–Al–P system exhibited a wider amorphous phase-forming range compared with the Ni–Al–P system.

3.2. Thermal stability

Changes in the exothermic peak on the DSC curve were examined for Fe–Al–P and Ni–Al–P amorphous alloys. The general features of the DSC curves for $Fe_{78}Al_4P_{18}$ and $Ni_{78}Al_4P_{18}$ alloys are shown in Fig. 2. The shape of the DSC curves indicates that the exothermic reaction of these alloys consists of two peaks even though no evident separation of the peaks is seen for the $Ni_{78}Al_4P_{18}$ alloy. A low intensity peak on the low temperature side results from the precipitation of the first crystalline phase from the amorphous phase and a narrow, high intensity peak on the high temperature side is due to the transition of the remaining amorphous phase to the second crystalline phase. Using X-ray diffraction study, it has been confirmed [5] that the first low peak was due to the precipitation of Fe(Al) crystals with a b c c structure for the Fe–Al–P system and Ni(Al) crystals with an f c c structure for the Ni–Al–P system and the second high peak due to the precipitation of an Fe_3P-type compound with an orthorhombic structure for the iron-based alloy and Ni_3P-type compound with an orthorhombic structure for the nickel-based alloy. Such a crystallization process via two stages (amorphous → amorphous + crystal-I → crystal-I + crystal-II) for X–Al–P (X = Fe or Ni) amorphous alloys is quite similar to that for X–Si–B [6, 7] and X–Al–B (X = Fe, Co or Ni) [1] amorphous alloys.

As shown in Fig. 1, the crystallization temperature T_x rises gradually with increasing aluminium and/or phosphorus content, and reaches 721 K for $Fe_{66}Al_{16}P_{18}$ and 628 K for $Ni_{78}Al_4P_{18}$. This indicates that the amorphous phase of the iron-based alloys is thermally more stable than that of the nickel-based alloys. Also, the most stable alloys against crystallization are located on the aluminium- and phosphorus-rich side in the amorphous phase-forming regions.

Additionally, the activation energy for crystallization was determined from the second exothermic peak corresponding to the precipitation of Fe_3P or Ni_3P compound on the DSC curve by the Kissinger method [6] because the majority of the exothermic heat for crystallization is occupied by the second peak. As shown in Fig. 3,

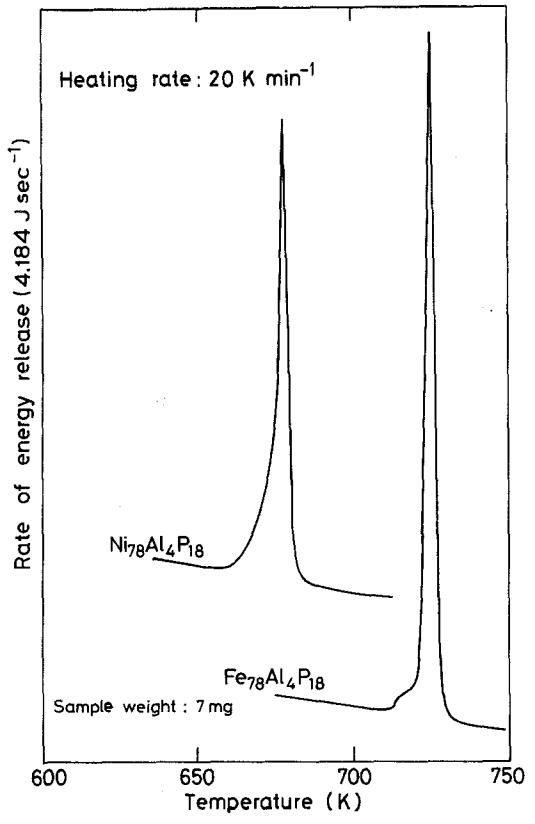

Figure 2 Differential scanning calorimetry curves for $Fe_{78}Al_4P_{18}$ and $Ni_{78}Al_4P_{18}$ amorphous alloys.

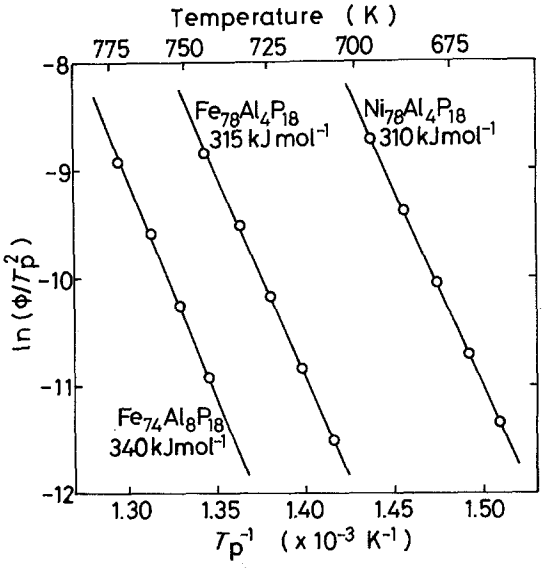

Figure 3 Kissinger plots of $\ln(\phi/T_p^2)$ against $1/T_p$ for $Fe_{78}Al_4P_{18}$, $Fe_{74}Al_8P_{18}$ and $Ni_{78}Al_4P_{18}$ amorphous alloys.

a linear relationship exists between $\ln(\phi/T_p^2)$ and $1/T_p$, where ϕ is the heating rate and T_p the temperature of the exothermic peak. The activation energy for crystallization is estimated to be about 315 kJ mol^{-1} for $Fe_{78}Al_4P_{18}$, 340 kJ mol^{-1} for $Fe_{74}Al_8P_{18}$ and 310 kJ mol^{-1} for $Ni_{78}Al_4P_{18}$. The energy is almost the same for the iron- and the nickel-based alloys which have the same aluminium and phosphorus compositions, despite the result that the T_x value is much higher for the former alloy than for the latter one. Judging from the results that the activation energy for crystallization is about 230 kJ mol^{-1} for $Fe_{82}P_{18}$ and 210 kJ mol^{-1} for $Ni_{82}P_{18}$ [5], it is concluded that the replacement of iron or nickel by aluminium results in a significant increase in the activation energy and hence the Fe–Al–P and Ni–Al–P alloys are more stable with respect to heating compared with the Fe–P and Ni–P alloys. It is well known that the crystallization of amorphous alloys occurs by a nucleation and growth process which is controlled by the diffusion of base metal. Therefore, it may be stated that the dissolution of the aluminium atom retards the diffusion of atoms in amorphous alloys.

3.3. Mechanical properties

The Vickers hardness (H_v) and tensile fracture strength (σ_f) of Fe–Al–P and Ni–Al–P amorphous alloys with a good bend ductility are shown in Figs. 4a and b, wherein the values marked with an asterisk are the tensile fracture strengths expressed in units of MPa. As seen in these figures, H_v increases gradually with the amount of aluminium or phosphorus present and reaches about 640 DPN for $Fe_{66}Al_{16}P_{18}$ and 545 DPN for $Ni_{78}Al_4P_{18}$. Thus, the higher value of hardness is obtained near the aluminium- or phosphorus-rich side of the amorphous phase-forming region. Also, the fracture strengths are about 1980 MPa for $Fe_{78}Al_4P_{18}$, 2020 MPa for $Fe_{74}Al_8P_{18}$ and 1910 MPa for $Ni_{78}Al_4P_{18}$. These strength values are rather lower than those for the X–Al–B [1] and X–Si–B [7, 8] (X = Fe, Co or Ni) alloys reported previously. Comparison of the hardness values (H_v) and fracture strengths (σ_f) between the Fe–Al–P and Ni–Al–P alloys shows that H_v and σ_f are much larger for the iron-based alloy than for the nickel-based alloy, as is the crystallization temperature. The ratio H_v/σ_f (DPN kg^{-1} mm^2) is almost equal to 3.0

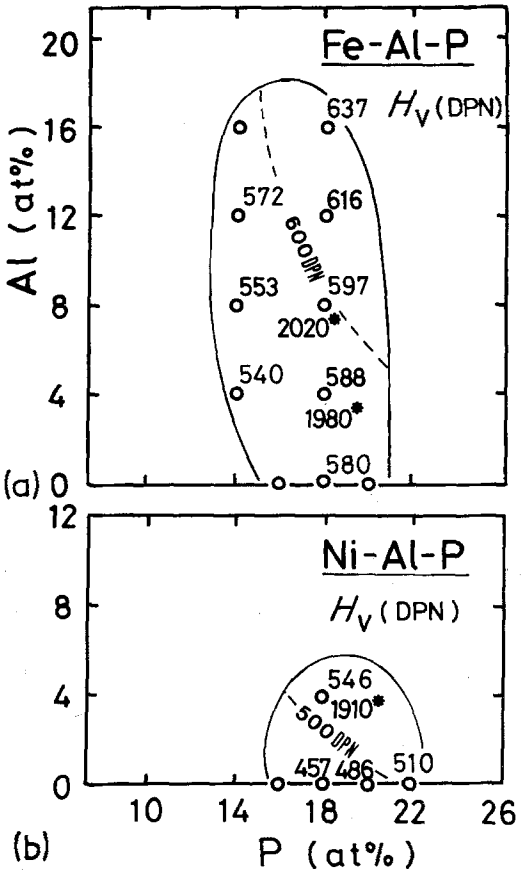

Figure 4 Changes in Vickers hardness and tensile fracture strength (σ_f) of the amorphous alloys with alloy composition. (a) Fe–Al–P system, (b) Ni–Al–P system.

as expected for amorphous alloys in which the indentation is accompanied with a large compressive plastic flow with little strain hardening [9].

3.4. Effect of aluminium on the hardness and crystallization temperature

From Figs. 1 and 4, it is clear that the variation of hardness and crystallization temperature with composition is similar for the two systems examined in the present experiment, namely, these values increase with increasing aluminium or phosphorus content. The increments in these values by the addition of 1 at% aluminium or phosphorus appear to be much greater for aluminium than for phosphorus. Here, the effectiveness of aluminium on the increase of crystallization temperature was compared with the data on the metalloid effect for iron-based alloys reported by Naka and Masumoto [10]. This result is shown

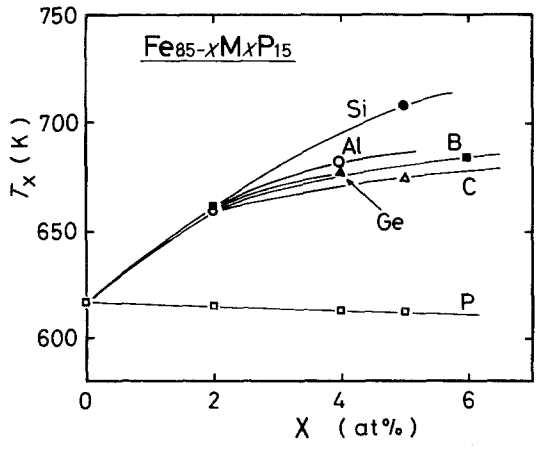

Figure 5 Effects of metalloid elements and aluminium on the crystallization temperature of $Fe_{85}P_{15}$ amorphous alloy.

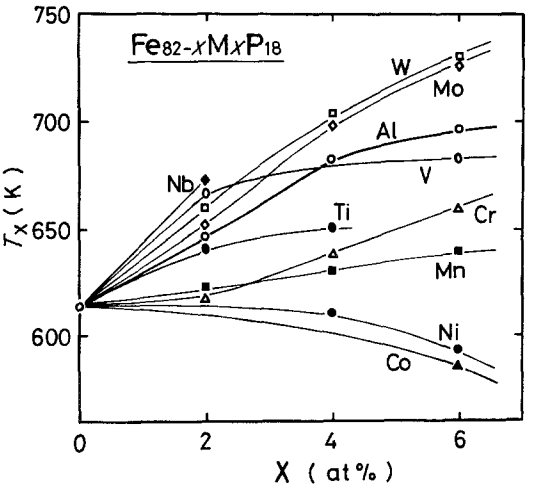

Figure 6 Effect of solute elements on the crystallization temperature of $Fe_{82}P_{18}$ amorphous alloy.

in Fig. 5. As seen in the figure, the effect of metalloids and aluminium on the increase of crystallization temperature decreases in the order of silicon > aluminium > boron ≃ germanium > carbon > phosphorus. Thus, the effect of aluminium is greater than that of all the metalloids except silicon. This result implies that the diffusion of atoms for crystallization is retarded by the dissolution of aluminium in spite of its low melting temperature. Such retardation appears to occur through the rather strong interaction between iron or nickel and aluminium, but the detailed mechanism remains unknown at present.

Additionally, the effect of aluminium on the crystallization temperature of Fe–P based amorphous alloys was compared with that of solute elements such as titanium, vanadium, niobium, chromium, molybdenum, tungsten, manganese, cobalt and nickel, as shown in Fig. 6. As seen in the figure, aluminium is a considerably effective element in raising the crystallization temperature despite the fact that aluminium is a soft metal with a low melting temperature. The effectiveness is almost the same order as that of refractory metals such as niobium, tungsten, molybdenum and vanadium, being much greater than that of titanium, chromium and manganese. On the other hand, the replacement of iron by cobalt or nickel results in a decrease in crystallization temperature.

The effects of solute elements (M = Ti, V, Nb, Cr, Mo, Co, Ni, Al, C or Si) on the activity coefficients γ_P^M of phosphorus in the molten iron saturated with phosphorus is shown in Fig. 7, where the slope of the straight lines corresponds to an interaction mother coefficient [11]. If the coefficient is negative, an attractive interaction acts between the phosphorus element and the solute element, while in the case of a positive coefficient a repulsive interaction acts between these elements. As seen in Fig. 7, since the titanium, vanadium, niobium, chromium or molybdenum element possesses a negative coefficient, an attractive interaction occurs between these elements and phosphorus. Consequently, it is considered that the rise in T_x by the replacement of iron with titanium, vanadium, niobium, chromium or molybdenum is due to a local short range ordering between the solute elements and the phosphorus element. On the other hand, a repulsive interaction generates between aluminium, silicon or carbon and phosphorus because of their positive coefficient. Nevertheless, the addition

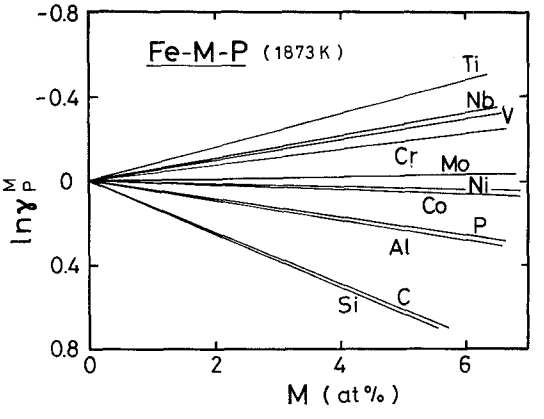

Figure 7 Effect of solute elements on the activity coefficient of phosphorus in molten iron.

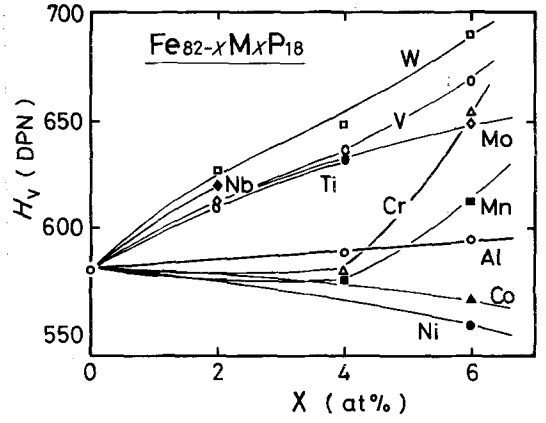

Figure 8 Effect of solute elements on the hardness of the $Fe_{82}P_{18}$ amorphous alloy.

of aluminium results in a significant increase in T_x as shown in Fig. 1. This result suggests that the increase in T_x is due to an attractive interaction between aluminium and iron, instead of an interaction between aluminium and phosphorus. Thus, the reason for the rise in T_x differs completely for the refractory metals and aluminium.

Additionally, the effect of solute elements on the hardness of Fe–P based amorphous alloys was compared with that of aluminium in Fig. 8. The effectiveness of aluminium is much lower than that of refractory metals such as tungsten, niobium, vanadium and molybdenum, in contrast to its great effectiveness in raising the crystallization temperature. This result implies that the replacement of iron by aluminium is very effective in retarding diffusion of atoms in amorphous alloys, but is less effective in increasing the bonding force among the constituent atoms. That is, it may be stated that the bonding of iron–aluminium and/or aluminium–phosphorus is weaker than that of iron–M and/or M-phosphorus for the case of M = titanium, vanadium, niobium, chromium, molybdenum or tungsten. Although such a contrast between crystallization temperature and hardness is observed in some amorphous alloys, the reason is still unknown at present. The detailed investigation on the atomic configuration in aluminium-containing amorphous alloys will shed some light on this problem.

4. Summary and conclusion

Ductile amorphous single phases containing aluminium have been found in the alloy systems of Fe–Al–P and Ni–Al–P by a melt-spinning technique. The aluminium content in these amorphous alloys is in the ranges 0 to18 at% for the Fe–Al–P system and 0 to 6 at% for the Ni–Al–P system. The crystallization temperature and hardness of these alloys increase with increasing aluminium and/or phosphorus content and the highest values attained are about 721 K and 640 DPN. The similar composition dependence of the activation energy for crystallization is also recognized. Also, their fracture strengths are of the order of 2000 MPa. The effectiveness of aluminium on the increment in crystallization temperature and hardness was compared with the previous data for other metals and metalloids. The addition of aluminium is very effective in raising the crystallization temperature, but is less effective in increasing hardness. The previous data on the effect of solute elements on the activity coefficient of phosphorus in molten iron indicate that a repulsive interaction acts between aluminium and phosphorus. It is therefore inferred that the increase in crystallization temperature and hardness by the dissolution of aluminium is due to the attractive interaction between iron or nickel and aluminium.

References

1. A. INOUE, A. KITAMURA and T. MASUMOTO, *J. Mater. Sci.* **16** (1981) 1895.
2. K. FUKAMICHI, M. KIKUCHI, H. HIROYOSHI and T. MASUMOTO, "Rapidly Quenched Metals III" Vol. 2, edited by B. Cantor (The Metals Society, London, 1978) p. 117.
3. T. MASUMOTO, K. HASHIMOTO and M. NAKA, "Rapidly Quenched Metals III" Vol. 2, edited by B. Cantor (The Metals Society, London, 1978) p. 435.
4. A. YOKOYAMA, H. KOMIYAMA, H. INOUE, T. MASUMOTO and H. M. KIMURA, *Scripta Met.* **15** (1981) 365.
5. A. KITAMURA, MSc, Tohoku University (1980).
6. H. E. KISSINGER, *Anal. Chem.* **29** (1957) 1702.
7. A. INOUE, T. MASUMOTO, M. KIKUCHI and T. MINEMURA, *J. Jap. Inst. Met.* **42** (1978) 294.
8. *Idem, Sci. Rep. Res. Inst. Tohoku Univ.* **A-27** (1979) 127.
9. R. HILL, "The Mathematical Theory of Plasticity" (Oxford University Press, London, 1967) p. 213.
10. M. NAKA and T. MASUMOTO, *Sci. Rep. Res. Inst. Tohoku Univ.* **A-27** (1979) 118.
11. "Metals Databook" (The Japan Institute of Metals, Maruzen, Tokyo, 1974). p. 94.

Received 28 May
and accepted 16 July 1982